Available online at website: https://jurnal.iaii.or.id/index.php/RESTI

JURNAL RESTI
(Rekayasa Sistem dan Teknologi Informasi)
Vol. 9 No. 4 (2025) 721 - 728 e-ISSN: 2580-0760

Face Dermatological Disorder Identification with YoloV5 Algorithm

Ayu Wirdiani[1*], Lennia Savitri Azzahra Lofiana[2], I Putu Arya Dharmadi[3], Oka Sudana[4]
[1,2,3,4]Teknologi Informasi, Fakultas Teknik, Universitas Udayana, Denpasar, Indonesia

[1]ayuwirdiani@unud.ac.id, [2]savitriazzahra@student.unud.ac.id, [3]aryadharmaadi@unud.ac.id, [4]agungokas@unud.ac.id

Abstract

Dermatological disorders are common in humans. The accurate identification of skin diseases is paramount for determining the most efficacious treatment. This system can screen images of skin diseases on the face and provide analysis results in the form of object detection. Dermatological disorders of the face are classified into six categories: acne nodules, melasma, filiform warts, milia, papules, and pustules. The YoloV5 algorithm was selected because of its effectiveness in live-detection tasks. The image-enhancement process involves the implementation of two methodologies: sharpening and histogram equalization. The former adjusts the brightness values whereas the latter adjusts the contrast values. The dataset comprised 1,223 images of skin diseases, with 947 images allocated for training and 276 for validation. The optimal mAP of the filiform wart class was determined to be 87.6%, with values of 76.7% for pustules, 72% for papules, 71% for milia, 68% for nodules, and 38.2% for melasma, representing the lowest value. The low mAP of melasma was attributed to the abstract image data type and complexity of localization. The congruence of object features and disparity in data variance has the potential to influence outcomes.

Keywords: computer vision; image enhancement; mean average precision; skin problems; YoloV5

How to Cite: Ayu Wirdiani, Lennia Savitri Azzahra Lofiana, I Putu Arya Dharmadi, and Oka Sudana, "Face Dermatological Disorder Identification with YoloV5 Algorithm ", *J. RESTI (Rekayasa Sist. Teknol. Inf.)* , vol. 9, no. 4, pp. 721 - 728, Jul. 2025.
*Permalink/*DOI: https://doi.org/10.29207/resti.v9i4.6237

Received: December 14, 2024
Accepted: June 17, 2025
Available Online: July 25, 2025

1. Introduction

The development of world technology is undergoing rapid improvement and change at an accelerated pace in various fields, including image processing and recognition. Image recognition and identification technology has found extensive application in the healthcare sector for the purpose of disease classification. The integration of sophisticated computer technology and artificial intelligence systems enables the expeditious and streamlined detection of diseases solely from visual imagery. The image is processed, thereby producing information in the form of disease types or information needs [1]. Dermatological disorders are problems or diseases that occur in the skin. It is a common disease in the world and affects millions of people. A plethora of cutaneous ailments are known to emerge under the influence of environmental factors, genetic predispositions, and traumatic injuries. [2]. The process of diagnosing cutaneous diseases is a complex undertaking, particularly when relying solely on visual cues. These visual indicators may include the morphology of the lesion, its distribution across the body, its pigmentation, the arrangement of the lesions, and the availability of diagnostic facilities [3]. The case study under consideration in this research specifically focused on a disorder in the facial skin area. The face is the part of the body that is most often given attention by many people, especially women, in matters of facial skin health and aesthetics. A range of dermatological conditions affecting the face are recognised, including dullness, dryness, acne, and cancer. The presence of a wide range of varied and intricate forms poses a significant challenge in the autonomous diagnosis of dermatological ailments [4]. Acne, a prevalent form of dermatological disorder, arises from the occlusion of inflamed pores within the oil glands. This obstruction leads to the formation of acne lesions [5], [6]. The various types of acne are categorised into blackhead, whitehead, pustule, nodule, and papule, depending on the form and severity of acne inflammation. Melasma is a condition characterised by an overproduction of melanin, the pigment responsible for skin colouration. This overproduction results in the appearance of dark patches on the skin. It is an established fact that fluctuations in skin condition may be observed over time. Such variations may be attributed to a number of factors, including external environmental influences, lifestyle choices, and the application of various skin

treatments. In addition to these exogenous factors, internal conditions such as hormonal imbalances may also contribute to skin condition fluctuations. The existing research on automatic acne classification using the deep residual neural network approach was utilised to classify five types of acne with AcneNet [7]. Detection technology has been used in a journal on the topic of skin problem detection with the Rethnet algorithm, and an MIoU result of 79.46% [8] was obtained. Another research used YoloV4 with the dataset used is DermNet NZ to recognize acne type with accuration 91,25% [9], also research that use R-CNN and Yolo for skin disease detection [10], research from [11] that used Deep Learning and Fuzzy Logic for diagnosis Melanoma Disease that achieve maximum accuration 88,64%. Yolov3 also used by [12] for diagnosis Melanoma Disease with Jac score of 86.12% and Dic of 92.55%.

The Computer Vision-based Face Dermatological Disorders Identification System with YoloV5 Algorithm is developed as a solution to detect human facial skin disease objects from six classes, such as acne nodules, black spots/melasma, filiform warts, milia, papules, and pustules. The main algorithm used to build this system to perform the identification process is the YoloV5 object detection algorithm. Yolo is a part of deep learning by utilizing CNN or an advanced Convolution Neural Network in its architecture. Research review from [13] that which compares several methods used in the recognition of skin diseases states the skin disease image recognition method based on deep learning is better than those of dermatologists and other computer-aided treatment methods. According to research on object recognition, Yolo performed the fastest during the research and successfully utilized conventional GPU [14] - [16]. YOLO, or You Only Look Once, is one of the algorithms developed aiming to perform object detection, especially on real-time objects [17] - [19]. The face dermatological disorder system can help the user to know the skin condition and its problems. This system is implemented with the aim of recognizing facial dermatological disorders based on the website with the YoloV5 algorithm. Thus, it can facilitate the user to do early detection and recognition independently of facial skin problems experienced. This system provides novelty, such as the construction of an object detection system for face dermatological disorders using YoloV5 so that input data can be dynamic images. The recognition results also provide localization so that if more than one type of facial skin disease appears, it can be distinguished by the user. This system is useful for people to recognize or detect facial skin diseases easily and independently. This research can be a reference and additional knowledge for developing diagnostic technology in the health sector with the help of computers for the community and technology developers.

2. Methods

The system overview in Figure 1 reveals the presence of two distinct flows. The training flow, delineated from 1-4, commenced with the collection of dermatological disorder image datasets from six classes: pustules, papules, nodules, filiform warts, melasma, and milia. The labeling process by giving a bounding box to the specified object class. The datasets that have been annotated were preprocessed automatically via a variety of image processing method, such as histogram equalization, sharpening, contrast adjustment, and brightness modification. The augmentation process was the stage to augment the data by providing treatment conditions, which was implemented after preprocessing. The data augmentation techniques implemented included rotation, flipping, shear, and brightness adjustments. The next stage of the process was the modeling and training stage, which began with the Yolov5 model pre-trained configuration utilizing the weight of the Yolo type. The determination of hyperparameters, including learning rate, batch size, epoch, weight decay, and optimizer, is conducted in accordance with the training needs. The last stage of the process is the training stage, during which the best weight model is stored.

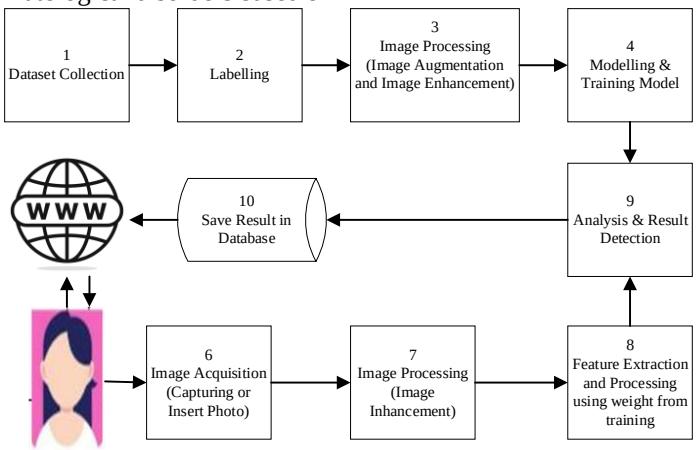

Figure 1. System Overview

The second flow was the flow from numbers 5-10, which represented system usage. The process was initiated with the user's image acquisition process, which provided input images from the camera or inserted images or videos. The input image would be processed through a preprocessing step that utilizes digital image processing techniques. The next stage was to perform feature extraction to obtain object detection results. The final stage of the system would provide output in the form of object detection results in the input image.

2.1 Datasets Collection

The collection and retrieval of data was conducted in order to fulfil the data requirements for the training process. The data was obtained from two distinct sources: the Skin 50-50 dataset and Google Images. Datasets were collected with each class in the form of training and validation data.

Table 1 is a training and validation dataset of six class data with 947 training and 276 testing data. Furthermore, datasets that have been collected will be manually labeled.

Table 1. Training and validation dataset

Variable Data	Training	Validation
Acne Nodules	198	53
Black Spots	138	43
Filiform Warts	140	52
Milia	137	39
Papules	136	38
Pustules	198	51
Total	947	274

2.2 Labeling

Labeling is defined as the process of marking and annotating objects according to a specific classification system. This process designated the class object's location to be acquired during the training process. The mark or label constituted a feature of the image, which was to be carried out in the feature extraction process in convolution. Figure 2 shown the labelling process.

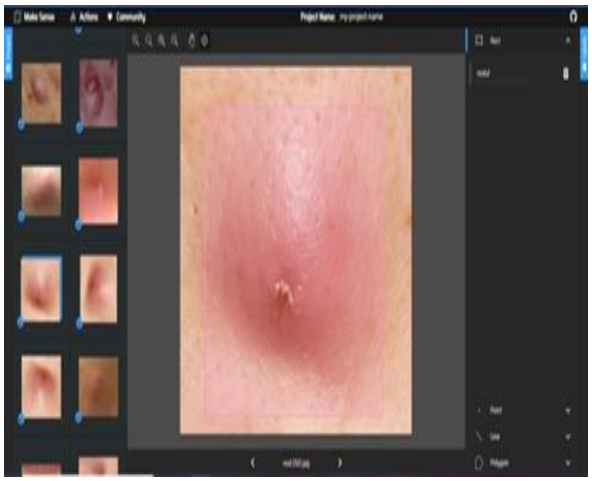

Figure 2. The labelling Process

2.3 Augmentation and Preprocessing

The image augmentation is a process that is used when there is a small amount of data and variance [20]. The data will be augmented by transforming the original image into different shapes in various ways. Figure 3 shown the process performed during augmentation. There was a vertical and horizontal flipping, rotation of -40 degrees and positive 40 degrees, shear of 10 degrees horizontal and 10 degrees vertical, 20% brightness, and reduced 20% brightness. The augmentation data was multiplied by 3x the amount of the original data.

The preprocessing process was used to improve image quality and prepare images for the training and detection process. Histogram colorization is a method used for the preprocessing process. This method finds the pixel color distribution value using alpha and beta values [21] [22]. The alpha value was obtained by dividing the value of 255 by the maximum gray minus the minimum gray. The beta value was obtained from the minimum gray multiplied by alpha. The alpha value represented the contrast value, and the beta value represented the brightness value. After testing and looking at various sources, the best alpha value threshold was around 1 to a maximum of 1.5. Even a slight shift in alpha value could change the contrast. The brightness value was set at a threshold of 40 and 60. Values outside the threshold would follow the closest limit to the threshold. The last preprocessing process was to increase the sharpen by 1.5.

2.4 The Training Process

The dataset that has been preprocessed will be train using pre-trained model from Yolov5. The processes in the YoloV5 architecture include convolution, pooling, bottleneck, upsampling and concatenate.

The training parameters used are 150 epochs, batch size 8 with an input image of 720x720. The model will be saved and used in the recognition process.

3. Results and Discussions

3.1 Training Results

The results of the training process are shown in Figure 4 using the Precision-Recall (PR) curve. A Precision-Recall (PR) curve is a plot that measures the performance of a Deep Learning model using precision and recall, which are performance metrics that evaluate the quality of a classification model. The curve is constructed with precision on the y-axis and recall on the x-axis. Figure 4 shown the result of training from six classes of face dermatological disorder. The highest value was filiform wart or kf, with 87.6%, and the lowest was melasma, at 38.2%. Other classes such as pustules were 76.7%, nodules 68.5%, papules 72%, and milia 71.1%. The reason why melasma had the lowest value because the data had abstract object patterns and varied color shapes and depths. It became a factor that made it more difficult for the machine to learn with the

melasma class than other classes. The amount of data and the data variance also affected how much mAP was generated. The accuracy results of the nodule, pustule, papule, and milia classes could still be improved. Improving accuracy could be done by adding data, performing more data variance, and data augmentation in the retraining process.

False Acceptance Rate (FAR) and False Rejection Rate (FRR) values can be seen in Figure 5. FAR value will be smaller when the threshold is getting bigger, while on the contrary, the FRR value is getting more significant when the threshold is getting bigger or directly proportional. The threshold value used was the threshold configuration of YoloV5 detection. Both FAR and FRR lines could determine the decision threshold or EER, the optimum threshold value to use. The optimum threshold could maintain the error rate of FAR and FRR. The accuracy rate of the system can be seen in Table 2.

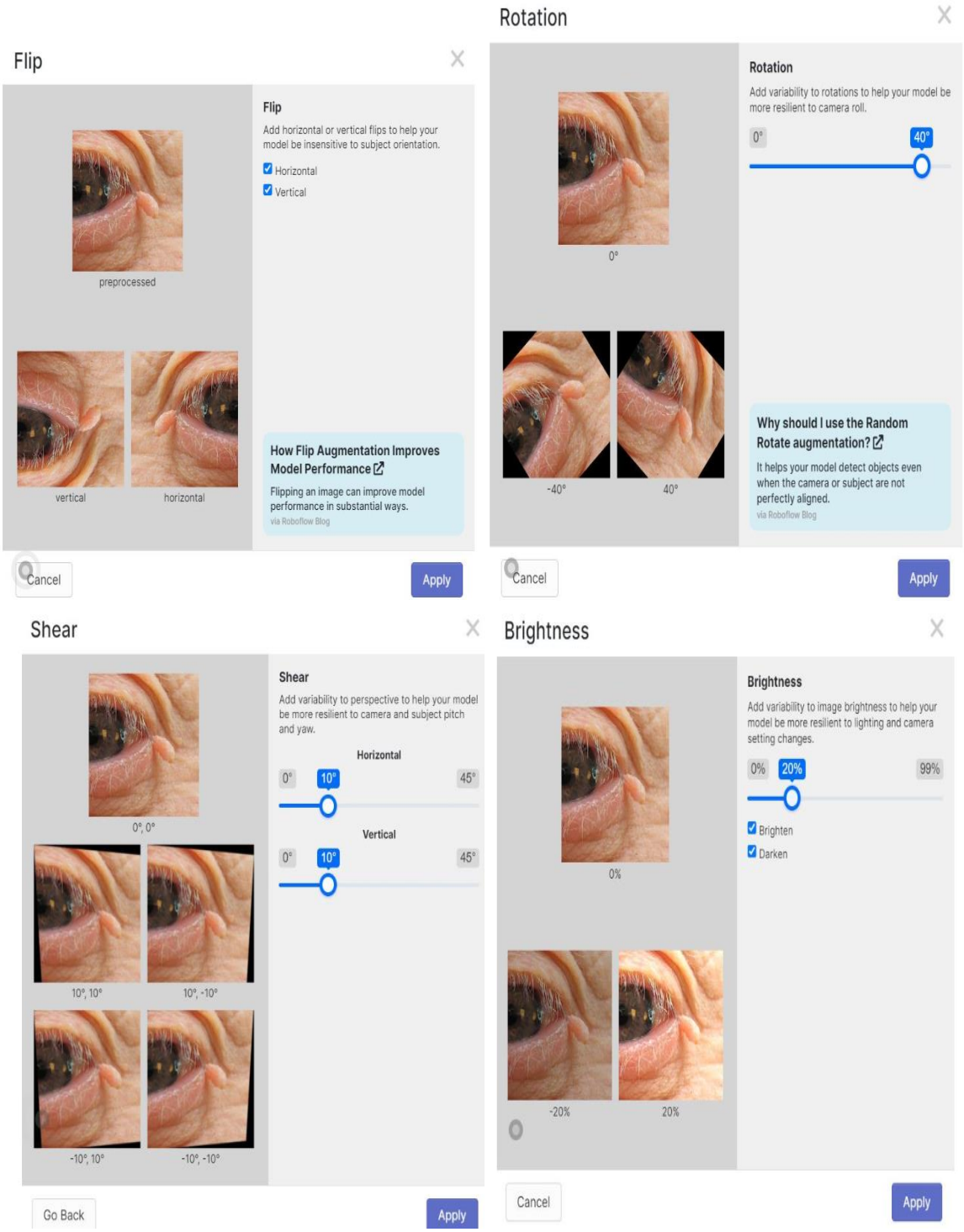

Figure 3. Augmentation Process

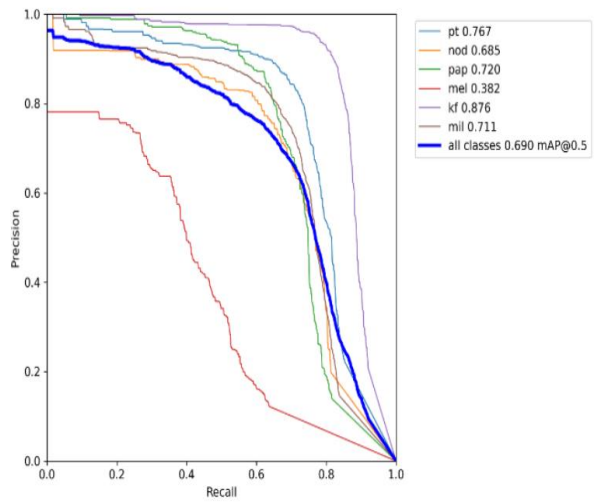

Figure 4. PR Curve Training

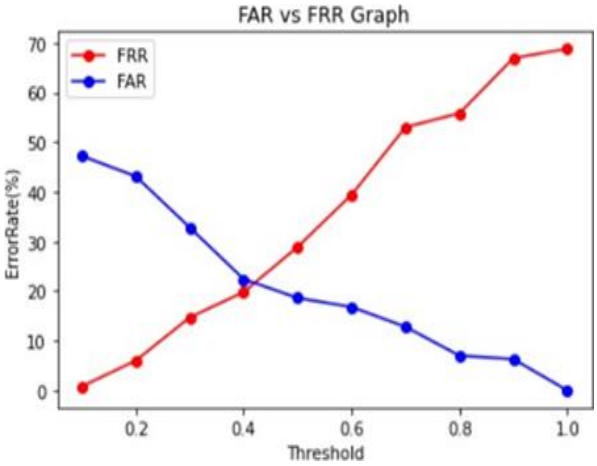

Figure 5. FAR FRR Graph

The optimum threshold value or EER from the closest FAR and FRR values is shown in Table 2. The FAR and FRR values at the best threshold were those with the lowest range. The best threshold value in the testing was 0.4, where FAR was 22.4% and FRR was 19.8%, which means there was an intersection on the graph at a point close to the 0.4 thresholds. Accuracy at threshold 0.4 was the highest, with 69%. The worst threshold value occurred at threshold 1, which had the furthest range, FAR 0% and FRR 68.8%, with an accuracy of 54.7%. The EER of the testing above was the value at the graph intersection, which was 21.1%.

Table 2. Accuracy rate

Threshold	Accuracy	FAR	FRR
0.1	56%	47.2	0.8
0.2	65.9%	43.1	6
0.3	67.8%	32.8	14.7
0.4	69%	22.4	19.8
0.5	67.1%	18.6	28.9
0.6	62%	16.8	39.4
0.7	60.4%	12.8	53
0.8	61.1%	7.6	55.8
0.9	54.8%	3	66.9
1	54.7%	0	68.8

The solution to obtain a lower error rate was to minimize FAR and FRR at the point of each class. FAR and FRR could occur due to the similarity of certain objects or features recognized during over-learning. Thus, a more detailed selection of training data on the features of each class can be done.

3.2. Face Dermatological Disorder Recognition Testing Results

The testing stage using two scenarios. The first scenarios were using image data that already preprocessing with the same class as the trained, such as filiform warts, milia, papules, pustules, and nodules. The second scenario used other skin disease data that had similarities with the six classes of skin diseases that had been trained. The testing results can be seen in Table 3.

The results show that out of 78 labeled objects from 11 images are detected, there are 67 objects and 11 undetected. The testing results show that the correct percentage is 84%. Undetected objects have weak characteristics such as small size, shape and color that are almost the same as skin color. The accuration value is based on the calculation of the confidence value. The confidence value is obtained from two values types such as the average accuration value of the class truth and the IoU value. IoU (Intersection over Union) is an accuracy metric between the predicted bounding box and the ground truth bounding box. The confidence value is a metric to measure the level of confidence or truth that the object selected by the bounding box is correct in a particular class.

In the second test scenario, the image with moles, pimples and skin diseases outside the training class is tested, details result shown in Table 4.

As shown in Table 4, moles were deted as filiform warts, but only one of the many moles was incorrectly detected. The other skin diseases such as Melanoma and Pimples that had similarities with the six class objects were undetected as the models that were trained. This was because the skin disease objects were outside the six training classes. Objects that have never passed the training process should not be detected according to testing in the experiment.

3.2 Website Testing Results

The last stage was website testing. It was used as a medium for conducting a face dermatological disorder test. The figure of input data options can be seen in Figure 7.

The options that could be selected were image input, video input, and real-time test input. The test process on the website required the user to register and log in. The image data input selection results can be seen in Figure 8.

Table 3. Test Scenario with Image Data Six Class Disease

Image Data	Undetected	Test Result
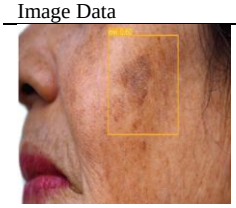	-	Melasma: 1
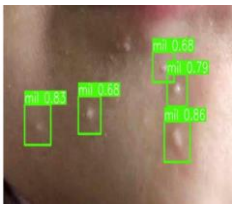	-	Millia: 5
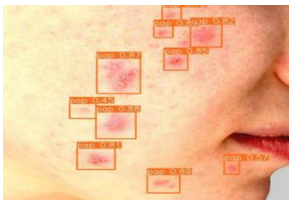	-	Papula: 10
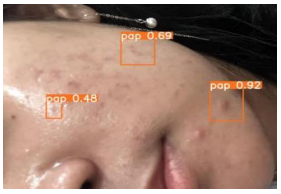	Nodul: 1 Papula: 1	Papula:3
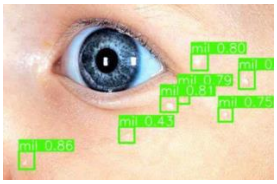	-	Milia: 7
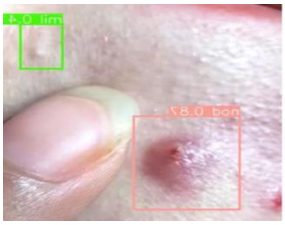	-	Nodul: 1 Milia: 1
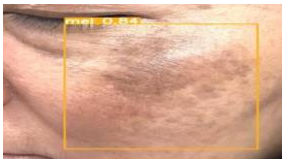	-	Melasma: 1
	filiform warts: 5	filiform warts: 13
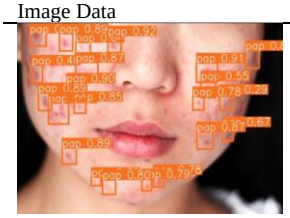	Papula: 3	Papula: 22
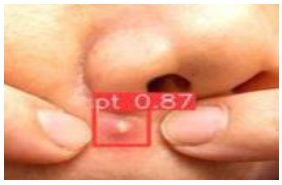	Pustula: 1	Pustula: 1
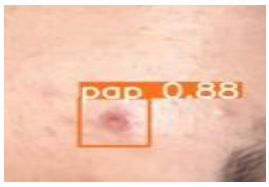	-	Papula: 1
Total	11	67

Table 4. Second Test Scenario with Image Data out of Six Class Disease

Image Data	Disease out class	Result
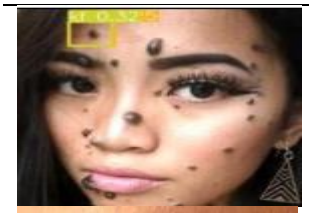	Moll	filiform warts: 1 with percentage: 0.32
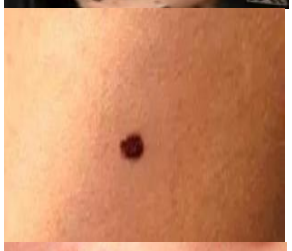	Moll	Undetected as six class disease
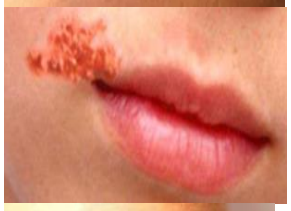	Melanoma	Undetected as six class disease
	Pimples	Undetected as six class disease

The results showed that the accuracy of papules was 26% and pustules was 86%. The image above was displayed on the result image page with id_result = 89. The results in video input can be seen in Figure 9.

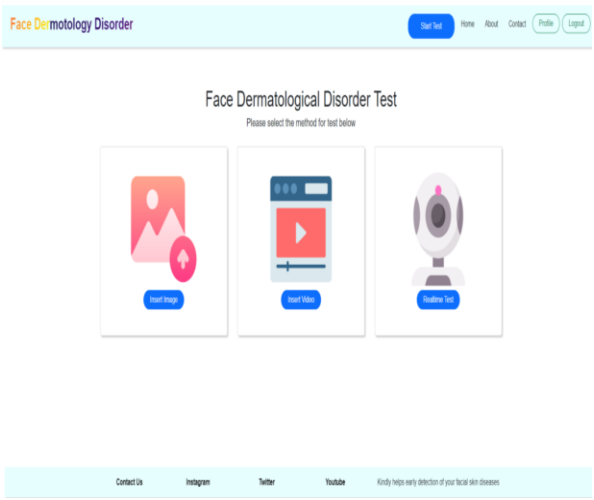

Figure 7. Option Selection Display

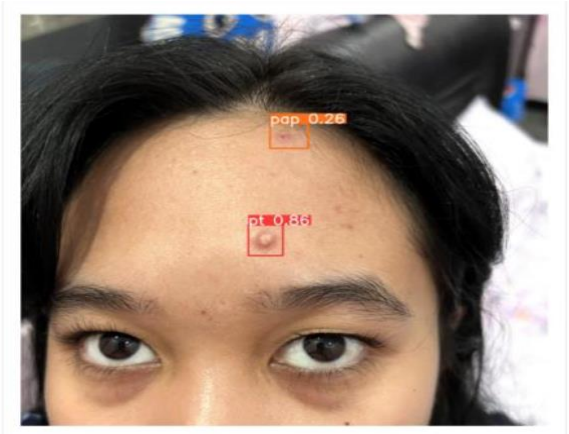

Figure 8. Testing Results of Processing Image Website

Figure 9. Processing Video Website Testing Results

The video showed that the accuracy of nodule-type acne is 93%, and other types of acne were detected, and it did not depend on the angle of shooting each fps. Video testing had a speed according to each user's device.

3.3 Analysis Comparison System

The comparison analysis of this research with similar and previous research was made using the system by Indah Widhi and Eri Zuliarso to detect facial skin diseases using TensorFlow lite. This library provides methods for using Convolutional Neural Networks [23]. This system had the advantage of detecting many types of skin diseases in as many as 20 classes and had good accuracy with 80% average accuracy. The disadvantage was that this system could not localize the skin disease area and could only classify it. Besides, the error percentage due to similar diseases was still quite large. Another comparison with an existing system utilizing computer vision application to assess the severity of acne disease on the face based on selfie data. The method used was a transfer learning approach with a ResNet 152 pre-trained model [24]. The data consisted of 4700 selfie images for training and 230 selfie images for testing. The advantage of this research was that the system could assess the severity of the disease with five severity levels: not acne, clear, almost creal, mild, moderate, and severe. The disadvantage was that this research was only limited to the type of acne disease and could still be improvised again. Research that had been done using the Yolo Method and Grabcut algorithm could segment skin lesions in dermoscopic images. This research aimed to perform early diagnosis of skin cancer by the system [25]. The challenge in this research was that the object segmentation medium used was dermoscopic images due to the large amount of noise, such as hair or water bubbles. The method used was the YoloV3 approach. It was used as an object detection algorithm to obtain the lesion location, which would be segmented. The advantage of this system was that it could perform the segmentation process, which was a more advanced level than detection, and the disadvantage was that there were still limited objects of skin disease lesions to be studied.

Research on Face Dermatological Disorder Identification Website System with YoloV5 Algorithm had conducted testing of six skin disease classes: pustules, papules, nodules, milia, filiform warts, and melasma. The testing process was divided into image data with the same class testing, image data with skin diseases outside of similar classes, and testing via the website. The overall testing results of this system successfully recognized facial skin diseases from the classes of pustules, papules, nodules, filiform warts, and milia. The melasma class had the lowest learning accuracy and the least good detection accuracy results among other classes. The average accuracy was 69%, where there was a difference in melasma accuracy with other classes. Thus, the overall class average value was low. The highest mAP accuracy value was filiform warts, with an accuracy of 87.6%, and the lowest was melasma at 38.2%. The mAP accuracy of the pustule class was 76.7%, nodule 68.5%, papule 72%, and milia 71.1%. Melasma could be a factor in decreasing accuracy. Melasma could be improvised by adding more data, variance the data, and data augmentation in the retraining process. The threshold value used was 0.4, which was obtained from finding the decision threshold of the FAR FRR graph.

4. Conclusions

This research concluded that the system could detect face dermatological disorders in six classes: pustules, nodules, papules, melasma, filiform warts, and milia. The mean Average Precission (mAP) value obtained was 69% with the highest value was in filiform warts at 87.6%, and the lowest was melasma at 38.2%. The testing used confidence value metrics obtained from the IoU value and object correctness accuracy to state whether the marked object was appropriate and relevant to its contents. The optimum threshold used based on the FAR FRR testing graph was at a threshold of 0.4 with the best accuration is 69%, FAR is 22.4% and FRR is 19.8%.

References

[1] S. K. Patnaik, M. S. Sidhu, Y. Gehlot, B. Sharma, and P. Muthu, "Automated skin disease identification using deep learning algorithm," *Biomed. Pharmacol. J.*, vol. 11, no. 3, pp. 1429–1436, 2018, doi: 10.13005/bpj/1507.

[2] H. W. Lim *et al.*, "The burden of skin disease in the United States," *J. Am. Acad. Dermatol.*, vol. 76, no. 5, pp. 958-972.e2, May 2017, doi: 10.1016/j.jaad.2016.12.043.

[3] Santhosh Kumar, C., Amritha Devangana, K., Abirami, P.L., Prasanna, M., Hari Aravind, S. (2023). Identification and Classification of Skin Diseases with Erythema Using YOLO Algorithm. In: Yadav, A., Nanda, S.J., Lim, MH. (eds) Proceedings of International Conference on Paradigms of Communication, Computing and Data Analytics. PCCDA 2023. Algorithms for Intelligent Systems. Springer, Singapore. https://doi.org/10.1007/978-981-99-4626-6_49.

[4] A. Aziz and K. Karpen, "Diagnosa Penyakit Kulit Wajah Menggunakan Metode Decission Tree Dan Algoritma C4.5," *J. Teknol. dan Open Source*, vol. 2, no. 1, pp. 74–86, 2019, doi: 10.36378/jtos.v2i1.148.

[5] W. N. Aini, N. Hidayah, and N. S. S. Ambarwati, "Pengurangan Jerawat Pada Kulit Wajah dengan Madu Manuka," *Pros. Semin. Nas. dan Call Pap.*, vol. 9, no. 1, 2019.

[6] E. Malgina and M.-A. Kurochkina, "Development of the Mobile Application for Assessing Facial Acne Severity from Photos," in *2021 IEEE Conference of Russian Young Researchers in Electrical and Electronic Engineering (ElConRus)*, Jan. 2021, pp. 1790–1793, doi: 10.1109/ElConRus51938.2021.9396382.

[7] M. S. Junayed *et al.*, "AcneNet - A deep CNN based classification approach for acne classes," 2019, doi: 10.1109/ICTS.2019.8850935.

[8] S. Bekmirzaev, S. Oh, and S. Yo, "RethNet: Object-by-object learning for detecting facial skin problems," 2019, doi: 10.1109/ICCVW.2019.00054.

[9] N. A. M. Isa and N. N. A. Mangshor, "Acne Type Recognition for Mobile-Based Application Using YOLO," *J. Phys. Conf. Ser.*, vol. 1962, no. 1, p. 012041, Jul. 2021, doi: 10.1088/1742-6596/1962/1/012041.

[10] S. Wulan Dari and J. Triloka, "Kajian Algoritme Mask Region-Based Convolutional Neural Network (Mask R-CNN) dan You Look Only Once (YOLO) Untuk Deteksi Penyakit Kulit Akibat Infeksi Jamur," *Semin. Nas. Has. Penelit. dan Pengabdi. Masy.*, 2022.

[11] S. Banerjee, S. K. Singh, A. Chakraborty, A. Das, and R. Bag, "Melanoma diagnosis using deep learning and fuzzy logic," *Diagnostics*, vol. 10, no. 8, 2020, doi: 10.3390/diagnostics10080577.

[12] S. Banerjee, S. K. Singh, A. Das, and R. Bag, "Diagnoses of Melanoma Lesion Using YOLOv3," in *Lecture Notes in Electrical Engineering*, 2022, vol. 786, doi: 10.1007/978-981-16-4035-3_26.

[13] L. F. Li, X. Wang, W. J. Hu, N. N. Xiong, Y. X. Du, and B. S. Li, "Deep Learning in Skin Disease Image Recognition: A Review," *IEEE Access*, vol. 8, 2020, doi: 10.1109/ACCESS.2020.3037258.

[14] Q. Aini, N. Lutfiani, H. Kusumah, and M. S. Zahran, "Deteksi dan Pengenalan Objek Dengan Model Machine Learning: Model Yolo," *CESS (Journal Comput. Eng. Syst. Sci.*, vol. 6, no. 2, p. 192, 2021, doi: 10.24114/cess.v6i2.25840.

[15] D. H. Fudholi, A. Kurniawardhani, G. I. Andaru, A. A. Alhanafi, and N. Najmudin, "YOLO-based Small-scaled Model for On-Shelf Availability in Retail," *J. RESTI (Rekayasa Sist. dan Teknol. Informasi)*, vol. 8, no. 2, pp. 265–271, 2024, doi: 10.29207/resti.v8i2.5600.

[16] Wirdiani, Ayu; Darma Putra, I Ketut Gede; Sudarma, Made; Sari Hartati, Rukmi; Savitri Azzahra Lofiana, "Real-time Face Recognition System Using Deep Learning Method," *Lontar Komput. J. Ilm. Teknol. Inf.*, vol. 14, no. 1, pp. 62–70, 2023, doi: https://doi.org/10.24843/LKJITI.2023.v14.i01.p06

[17] L. You, Y. Ke, H. Wang, W. You, B. Wu, and X. Song, "Small traffic sign detection and recognition in high-resolution images," in *Lecture Notes in Computer Science (including subseries Lecture Notes in Artificial Intelligence and Lecture Notes in Bioinformatics)*, 2019, vol. 11518 LNCS, doi: 10.1007/978-3-030-23407-2_4.

[18] A. N. Kadhum and A. N. Kadhum, "Literature Survey on YOLO Models for Face Recognition in Covid-19 Pandemic," *J. Image Process. Intell. Remote Sens.*, no. 34, 2023, doi: 10.55529/jipirs.34.27.35.

[19] Mohammad Chasrun Hasani, Fadhila Milenasari, and N. Setyawan, "Pemantauan Physical Distance Pada Area Umum Menggunakan YOLO Tiny V3," *J. RESTI (Rekayasa Sist. dan Teknol. Informasi)*, vol. 6, no. 1, pp. 146–152, 2022, doi: 10.29207/resti.v6i1.3808.

[20] J. Ma, C. Hu, P. Zhou, F. Jin, X. Wang, and H. Huang, "Review of Image Augmentation Used in Deep Learning-Based Material Microscopic Image Segmentation," *Appl. Sci.*, 2023, doi: 10.3390/app13116478.

[21] F. W. Gandhi and L. Lina, "Pengenalan Jenis Maker Dengan Metode Color Histogram Dan Euclidean Distance," *J. Ilmu Komput. dan Sist. Inf.*, vol. 9, no. 2, p. 18, 2021, doi: 10.24912/jiksi.v9i2.13100.

[22] C. P. Beauty and Y. A. Sari, "Temu Kembali Citra Makanan Menggunakan Color Histogram Dan Local Binary Pattern," *J. Pengemb. Teknol. Inf. dan Ilmu Komput.*, vol. 3, no. 6, pp. 5514–5520, 2019.

[23] I. W. Prastika and E. Zuliarso, "Deteksi Penyakit Kulit Wajah Menggunakan Tensorflow Dengan Metode Convolutional Neural Network," *J. Manaj. Inform. dan Sist. Inf.*, vol. 4, no. 2, 2021, doi: 10.36595/misi.v4i2.418.

[24] Z. Ren, K. Qian, Z. Zhang, V. Pandit, A. Baird and B. Schuller, "Deep Scalogram Representations for Acoustic Scene Classification," in IEEE/CAA Journal of Automatica Sinica, vol. 5, no. 3, pp. 662-669, May 2018, doi: 10.1109/JAS.2018.7511066.

[25] H. M. Ünver and E. Ayan, "Skin lesion segmentation in dermoscopic images with combination of yolo and grabcut algorithm," *Diagnostics*, vol. 9, no. 3, 2019, doi: 10.3390/diagnostics9030072.